Polymer 50 (2009) 5661–5667

Contents lists available at ScienceDirect

Polymer

journal homepage: www.elsevier.com/locate/polymer

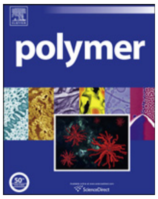

Effects of the oil–water interface on network formation in nanogel synthesis using nitroxide-mediated radical copolymerization of styrene/divinylbenzene in miniemulsion

Per B. Zetterlund*, Nur Alam [1], Masayoshi Okubo**

Department of Chemical Science and Engineering, Graduate School of Engineering, Kobe University, Kobe 657-8501, Japan

ARTICLE INFO

Article history:
Received 25 August 2009
Received in revised form
1 October 2009
Accepted 6 October 2009
Available online 9 October 2009

Keywords:
Nitroxide-mediated polymerization
Crosslinking
Miniemulsion

ABSTRACT

Nitroxide-mediated radical copolymerization of styrene (99 mol%)/divinylbenzene (1 mol%) employing the nitroxide 2,2,6,6-tetramethylpiperidinyl-1-oxy (TEMPO) in aqueous miniemulsion using sodium dodecylbenzenesulfonate as surfactant has been carried out at 125 °C. At a given styrene conversion, the degree of crosslinking increases with decreasing polystyrene–TEMPO macroinitiator concentration in excess of what is predicted based on the increase in primary chain length assuming an ideal controlled/living process. This discrepancy is mainly a result of the oil–water interface effect on the deactivation reaction between propagating radicals and TEMPO. This interface effect causes a marked increase in primary chain length, and therefore an accompanying increase in the number of crosslinks per primary chain. Polymerizations in the presence of free TEMPO minimizes the interface effect, and one then obtains molecular weight distributions and well-defined networks conducive with a controlled/living process.

1. Introduction

The advent of controlled/living radical polymerization (CLRP) [1] has made it possible to synthesize crosslinked nanoparticles (nanogels) with unprecedented control over the network in terms of macromolecular structure and homogeneity [2,3]. In short, the combination of CLRP and crosslinking chemistry (e.g. copolymerization of monovinyl/divinyl monomer) leads to the formation of more homogeneous networks without microgels, higher swelling and anticipated superior mechanical properties [4–12]. Crosslinking CLRP in dispersed systems [2] thus offers an attractive route to nanogels with a range of applications, e.g. drug-delivery [13].

Nitroxide-mediated radical polymerization (NMP) [14,15] is the oldest of the well-established techniques for CLRP, based on the reversible deactivation of propagating radicals by nitroxide. NMP in aqueous miniemulsion has been studied extensively over the past decade [2,16,17]. The most extensively studied system is the 2,2,6,6-tetramethylpiperidinyl-1-oxy (TEMPO)-mediated polymerization of styrene (S), which can proceed under significant influence of various intrinsic heterogeneous features such as compartmentalization [18–21], interface effects on the deactivation reaction [22–25] and enhanced spontaneous radical generation [26,27]. The effects of these specific features on the network development in crosslinking NMP in aqueous miniemulsion are poorly understood.

We have previously reported an interface effect on the deactivation reaction in TEMPO-mediated miniemulsion polymerization of S at 125 °C, according to which some fraction of TEMPO is located near/adsorbed at the interface, leading to a reduction in deactivation rate, higher polymerization rate (R_p) and (partial) loss of control/livingness [22–25]. Enhanced spontaneous (thermal) initiation of S related to the oil–water interface [27], as well as radical generation involving the surfactant sodium dodecylbenzenesulfonate (SDBS) [26], may also lead to increased R_p relative to bulk in S/TEMPO miniemulsion. More recently, we have reported that the control/livingness in NMP of S in aqueous miniemulsion at 125 °C employing a PS–TEMPO macroinitiator depends strongly on the macroinitiator concentration for sufficiently small particles [25]. The control/livingness was relatively poor at $[\text{PS–TEMPO}]_0 \le 0.02$ M due to the combined effect of the interface effect on the deactivation reaction and enhanced spontaneous initiation, whereas satisfactory control/livingness was obtained at $[\text{PS–TEMPO}]_0 > 0.02$ M, i.e. the effects of the interface decrease with increasing macroinitiator concentration.

---

* Corresponding author. Centre for Advanced Macromolecular Design (CAMD), School of Chemical Sciences and Engineering, The University of New South Wales, Sydney, NSW 2052, Australia. Tel.: +61 2 9385 4331; fax:+61 2 9385 6250.
** Corresponding author. Tel./fax: +81 78 803 6161.
E-mail addresses: p.zetterlund@unsw.edu.au (P.B. Zetterlund), okubo@kobe-u.ac.jp (M. Okubo).
[1] Pulp and Paper Research Centre, Department of Chemistry, McGill University, Montreal, Canada.

0032-3861/$ – see front matter © 2009 Elsevier Ltd. All rights reserved.
doi:10.1016/j.polymer.2009.10.012

In the case of the TEMPO-mediated radical crosslinking copolymerization of S and divinylbenzene (DVB) in aqueous miniemulsion at 125 °C, the apparent pendant reactivity (i.e. the crosslink density) [6,8,28] increased and the gel-point was lower [29,30] in the presence of the hydrophobe tetradecane. Poly(DVB) is known to migrate to the interface of monomer/toluene droplets in an aqueous emulsion, and this process is promoted by the presence of a hydrophobe such as hexadecane [31]. This is the basis of the self-assembling of phase separated polymer (SaPSeP) method for hollow polymer particle synthesis [32–34]. Subsequent work employing TEMPO-based interfacially active macroinitiators of various hydrophilicity comprising S and methyl acrylate showed that the pendant conversion is strongly influenced by the macroinitiator hydrophilicity. The interfacially active macroinitiators are to some extent preferentially adsorbed at/located near the oil–water interface, which results in an increase in the ratio [pendant unsaturation]/[monomer] in the vicinity of propagating radicals, and thus an increase in pendant conversion. Furthermore, the pendant conversion increased with decreasing particle size due to this interface effect (not to be confused with the interface effect on deactivation) increasing in significance with increasing total interfacial area of the system.

The aim of the present study has been to further probe how the three-dimensional polymer network development during TEMPO-mediated radical crosslinking polymerization is influenced by the oil–water interface via the interface effect on deactivation and enhanced spontaneous radical generation originating at the interface. To this end, TEMPO-mediated copolymerizations of S and DVB have been performed at 125 °C in aqueous miniemulsion employing various PS–TEMPO macroinitiatior concentrations, and with and without free TEMPO.

2. Experimental section

2.1. Materials

S was purified by distillation under reduced pressure in a nitrogen atmosphere. DVB (Nippon steel chemical; purity 99%) was washed with 1 N NaOH and distilled water to remove inhibitors. Benzoyl peroxide (BPO) was purified by recrystallization using chloroform/methanol, TEMPO (Aldrich), and sodium dodecylbenzenesulfonate (SDBS; Nacalai Tesque Inc., Kyoto, Japan) were used as received.

2.2. Preparation of macroinitiator

PS–TEMPO: S (13.5 g), BPO (371 mg; 0.103 mol L^{-1}) and TEMPO (285 mg; 0.122 mol L^{-1}) were charged in a glass tube, degassed with several N_2 cycles, sealed off under vacuum and heated at 125 °C for 4 h in an oil bath. The polymer was recovered by precipitation in excess methanol, and subsequently purified by reprecipitation four times using toluene/methanol and dried in a high vacuum oven. S conversion = 18%, $M_n = 2250$, $M_w/M_n = 1.19$.

2.3. Polymerization procedures

Miniemulsion polymerizations (5.0 wt% solids content based on 100% monomer conversion): A solution of styrene (S; 0.7405 g; 99 mol% rel. to total monomer), DVB (9.5 mg; 1 mol% rel to total monomer), PS–TEMPO macroinitiator (0, 11, 44, 88, 132 mg; 0, 5, 20, 40, 60 mmol L-monomer^{-1}), was mixed with an aqueous solution of dodecyl benzenesulfonic acid sodium salt (SDBS; 45 mg; 6 wt% rel. to total monomer). Miniemulsion polymerization containing free TEMPO was the same as above except that TEMPO (5 mol% rel. to total PS–TEMPO) was added.

Emulsification was carried out using ultrasonication (Ultrasonic Homogenizer, Nissei, US-600T) for 12 min at 0 °C. The resulting emulsions were transferred to glass ampules (each ampule contained approximately 4 mL), degassed using several N_2/vacuum cycles and sealed off under vacuum, and the reactions were carried out at 125 °C shaking the ampules horizontally at a rate of 110 cycles/min.

2.4. Measurements

Particle size distributions were measured using dynamic light scattering (FPAR-1000, Otsuka Electronics, Osaka, Japan) at the light scattering angle of 160° at room temperature. Number-average (d_n) and weight-average (d_w) droplet diameters (given in Fig. captions) were obtained using the Marquadt analysis routine. The values given are average values over the course of the polymerizations.

S and DVB conversions were determined by gas chromatography (Shimadzu Corporation, GC-18A) with helium as carrier gas, employing *N,N*-dimethylformamide as solvent and *p*-xylene as internal standard.

Molecular weight distributions (MWDs) were obtained by gel permeation chromatography (GPC) employing a Tosoh GPC system equipped with two TSK gel columns (GMHHR-H, 7.8 mm i.d. ×30 cm) using tetrahydrofuran (THF) as eluent at 40 °C at a flow rate of 1.0 mL min^{-1}, and a refractive index detector (RI-8020). The column was calibrated against five standard polystyrene samples (1.05×10^3–5.48×10^6 g/mol). All polymer samples were soluble in THF.

^{1}H NMR spectra, for estimation of pendant conversions as described previously [8], were recorded on a Bruker (Avance-500) spectrometer (Karlsruhe, Germany) with deuteriochloroform and hexamethyldisiloxane as solvent and internal standard, respectively. The polymer concentration was approximately 10 wt%. The polymer was collected by oven drying followed by reprecipitation using toluene/methanol to ensure complete removal of residual monomer.

3. Results and discussion

3.1. Rate of polymerization

Fig. 1 shows conversion vs. time data for TEMPO-mediated radical copolymerizations of S and DVB in miniemulsion using SDBS as colloidal stabilizer and in bulk at 125 °C using different concentrations of PS–TEMPO macroinitiator (0–60 mM). R_p increased quite dramatically with decreasing [PS–TEMPO]$_0$ (0–60 mM) for miniemulsions at similar particle size ($d_n \approx 65$ nm), exhibiting much higher R_p than the bulk system with [PS–TEMPO]$_0$ = 20 mM. This trend is similar to what has been observed and discussed in detail previously for the corresponding linear polymerization of S (i.e. no DVB) at different [PS–TEMPO]$_0$ [25]. In short, R_p is higher for smaller particles as a combined result of the interface effect on the deactivation reaction [22–25] and the enhanced rate of spontaneous initiation in aqueous dispersed S systems [27]. The interface effect on deactivation refers to some fraction of the free TEMPO residing at/near the oil–water interface, thus giving a reduction in the deactivation rate. A reduction in [PS–TEMPO]$_0$ corresponds to a reduction in TEMPO concentration, and if the TEMPO concentration is low, the interface effect on the deactivation reaction becomes more significant (greater interfacial area per TEMPO molecule). Likewise, the lower the TEMPO concentration (i.e. the lower [PS–TEMPO]$_0$), the greater the effect of spontaneously generated radicals on R_p, because less TEMPO is available to capture the extra radicals. It may appear odd that R_p increases with decreasing macroinitiator concentration, despite the heterogeneous effects outlined above. However, recall that in bulk, R_p for the linear system (no DVB) is independent of [PS–TEMPO]$_0$ [35].

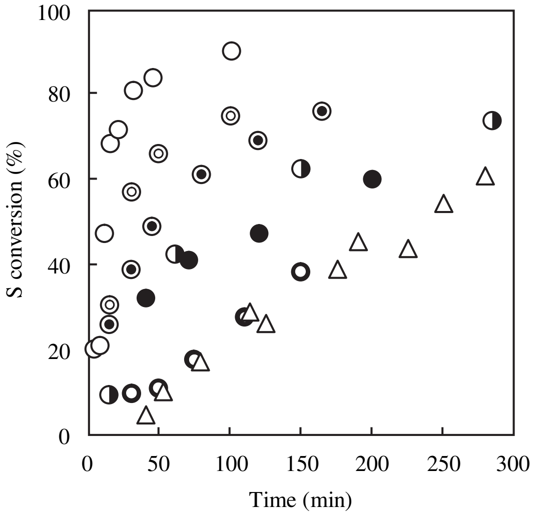

Fig. 1. Conversion-time plots based on S for TEMPO-mediated copolymerization of S and DVB (1 mol%) at 125 °C in miniemulsion and bulk at various PS–TEMPO macroinitiator concentrations: Miniemulsion: $[\text{PS–TEMPO}]_0 = 0$ M (○; $d_n \approx 64$ nm; $d_w \approx 72$ nm), 5 mM (◎; $d_n \approx 65$ nm; $d_w \approx 86$ nm), 20 mM (◉; $d_n \approx 65$ nm; $d_w \approx 85$ nm,**O**; $d_n \approx 1000$ nm; $d_w \approx 1300$ nm), 40 mM (◑; $d_n \approx 62$ nm; $d_w \approx 74$ nm), 60 mM (●; $d_n \approx 56$ nm; $d_w \approx 68$ nm). Bulk: $[\text{PS–TEMPO}]_0 = 20$ mM (△).

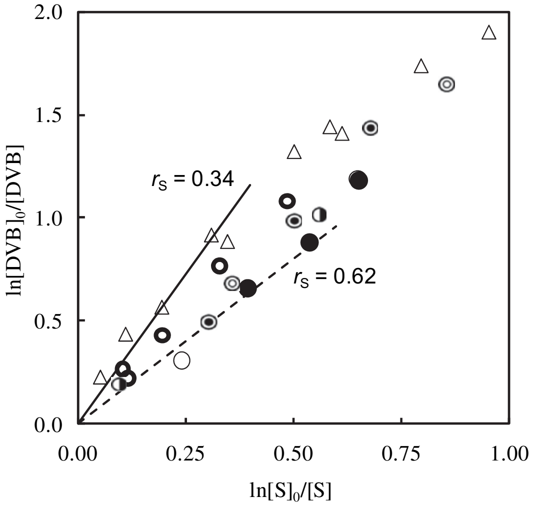

Fig. 2. Relative rates of S and DVB consumption expressed as $\ln[\text{DVB}]_0/[\text{DVB}]$ vs. $\ln[\text{S}]_0/[\text{S}]$ for TEMPO-mediated copolymerization of S and DVB (1 mol%) at 125 °C in miniemulsion and bulk at various PS–TEMPO macroinitiator concentrations. The lines are best fits at low conversion based on Eq. (1) (see text for details). The legend is the same as in Fig. 1.

Fig. 1 also shows data for the larger particle size of $d_n \approx 1000$ nm at $[\text{PS–TEMPO}]_0 = 20$ mM, revealing that R_p was much lower than for $d_n \approx 65$ nm, and very close to R_p in bulk as observed previously for the corresponding system without DVB [22,23]. The greater the particle size, the smaller is the overall interfacial area of the system, and thus the smaller are the interface effect on deactivation and enhanced spontaneous radical generation (the enhanced radical generation is likely originating at the interface [27]).

Compartmentalization can significantly affect NMP in dispersed systems if the particles are sufficiently small and/or $[\text{PS–TEMPO}]_0$ is sufficiently low [18–21]. According to theory, compartmentalization for S/TEMPO/125 °C is important for $d < 65$ nm for $[\text{PS–TEMPO}]_0 = 20$ mM. The effect would be a reduction in R_p relative to the corresponding bulk system due to the confined space effect on deactivation. For $[\text{PS–TEMPO}]_0 < 20$ mM, compartmentalization effects may be at play [19]. However, it is apparent that with regards to R_p, the interface effect on deactivation and enhanced spontaneous radical generation are dominant factors.

3.2. *DVB consumption*

The build-up of the polymer network is influenced by the rate of consumption of DVB relative to that of S, which can be estimated based on Eq. (1):

$$\ln\frac{[\text{DVB}]_0}{[\text{DVB}]} = \frac{1}{r_S}\ln\frac{[\text{S}]_0}{[\text{S}]} \tag{1}$$

where r_S is the styrene monomer reactivity ratio (based on the rate coefficient ratio $k_{\text{S-S}}/k_{\text{S-DVB}}$). The validity of Eq. (1) rests on the fact that the vast majority of propagation steps involve S-terminated radicals ($[\text{S}]_0 >> [\text{DVB}]_0$) [6].

Plotting the data according to Eq. (1) reveals that the rate of consumption of DVB relative to that of S was higher in bulk than in miniemulsion (Fig. 2), and decreased with decreasing particle size (compare $d_n \approx 65$ and 1000 nm for $[\text{PS–TEMPO}]_0 = 20$ mM). Within experimental error, no clear trend can be discerned with regards to any effects of $[\text{PS–TEMPO}]_0$ on the relative monomer consumption rates. Fitting of Eq. (1), excluding the data at high conversion, resulted in $r_S = 0.34$ in bulk, and a maximum value of $r_S = 0.62$ for the miniemulsion with $d_n \approx 56$ nm and $[\text{PS–TEMPO}]_0 = 60$ mM, which lie within the range of values reported in the literature [36]. The tendency for the apparent value of r_S to decrease with increasing particle size (the bulk system representing "infinite particle size") has been observed previously for this system, but remains to be clarified mechanistically [6,8].

These differences in r_S will exert a strong influence on the distribution of DVB units, i.e. potential crosslinks, along the polymer backbone (primary chains), and therefore ultimately on the final network structure. The instantaneous copolymer composition for $r_S = 0.34$ and 0.62 was calculated using numerical integration of Eqs. (2) and (3) using arbitrary input values for $k_{\text{S-S}}$, $k_{\text{S-DVB}}$ and $[\text{PS}^{\bullet}]$ [37].

$$\mathrm{d}[\text{DVB}]/\mathrm{d}t = -k_{\text{S-DVB}}[\text{PS}^{\bullet}][\text{DVB}] \tag{2}$$

$$\mathrm{d}[\text{S}]/\mathrm{d}t = -k_{\text{S-S}}[\text{PS}^{\bullet}][\text{S}] \tag{3}$$

The instantaneous composition is governed solely by the relative consumption rates of S and DVB, and thus the absolute values of $k_{\text{S-S}}$, $k_{\text{S-DVB}}$ and $[\text{PS}^{\bullet}]$ do not influence the result. The treatment rests on the same assumptions as Eq. (1) above. The results are presented as the number of S units between DVB units (N_S; potential branching points) (Fig. 3). The initial value of N_S is lower for $r_S = 0.34$ than 0.62 due to the higher relative apparent reactivity of DVB, whereas at higher S conversion the trend is the reverse as a result of the monomer mixture becoming gradually depleted of DVB. From the viewpoint of crosslink distribution along the primary chains, the network would be more homogeneous for the miniemulsion systems with $d_n = 65$ nm ($r_S \approx 0.62$) than for the bulk system ($r_S = 0.34$).

3.3. *Pendant conversions*

The pendant conversion is defined as the conversion at any point in time of the pendant unsaturations incorporated into the polymer via reaction of DVB units, that is, a pendant conversion of 50% means that half of the DVB units in the polymer constitute crosslinks. Fig. 4 shows the pendant conversions vs S conversion for miniemulsions with $d_n \approx 65$ and 1000 nm and different

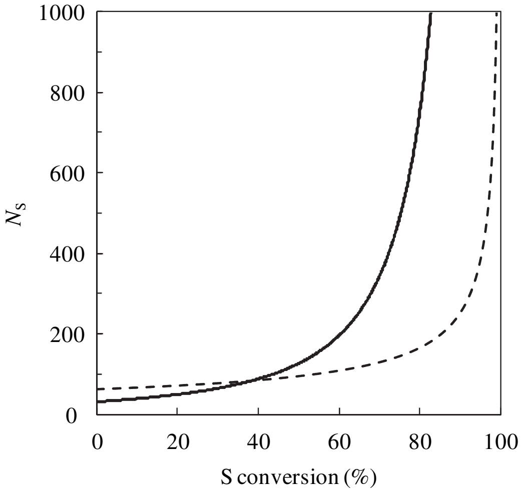

Fig. 3. Plot of the number of S units between potential crosslinks (N_S) at different S conversions calculated from Eqs. (2) and (3) for $r_S = 0.34$ (full line) and 0.62 (dotted line). See text for details.

[PS–TEMPO]$_0$ corresponding to the data in Fig. 1. For all polymerizations, the pendant conversions increased with increasing S conversion over the conversion range investigated.

The pendant conversions are markedly higher for $d_n \approx 65$ than 1000 nm, regardless of [PS–TEMPO]$_0$. This trend with particle size has been reported previously for the present system [6,8], and is believed to be related to migration of polymer to the oil–water interface. This would cause an increase in the ratio [pendant unsaturation]/[monomer] in the vicinity of propagating radicals, resulting in an increase in the apparent pendant reactivity [6,8,29,30,38].

Although there is considerable scatter, it appears that the pendant conversion is relatively independent of [PS–TEMPO]$_0$. A decrease in [PS–TEMPO]$_0$ results in an increase in primary chain length. The primary chain length refers to the chain length if all crosslinks were severed, i.e. the chain length of the corresponding system where DVB has been replaced by S, and can be estimated as $M_{n,th} = (\alpha[M]_0 M_M)/[TEMPO]_0$, where α is the total monomer conversion, $[M]_0$ denotes the total monomer concentration, and M_M can be approximated as the MW of S. Longer chains may result in lower pendant reactivity due to steric effects [39]. However, longer chains would lead to an increased pendant concentration in the vicinity of the radical chain end, and thus higher apparent pendant reactivity due to enhancement of intramolecular reaction [4,40]. The net effect would depend on the relative importance of the two contributions and cannot be readily predicted.

However, even though the pendant conversions are similar irrespective of [PS–TEMPO]$_0$, it is important to realize that the crosslink density would increase with decreasing [PS–TEMPO]$_0$ as a result of the corresponding increase in primary chain length (thus a higher number of crosslinks per chain). In the present system, $M_{n,th} \approx 44{,}000\ \mathrm{g\,mol^{-1}}$ at 100% monomer conversion for [PS–TEMPO]$_0$ = 20 mM.

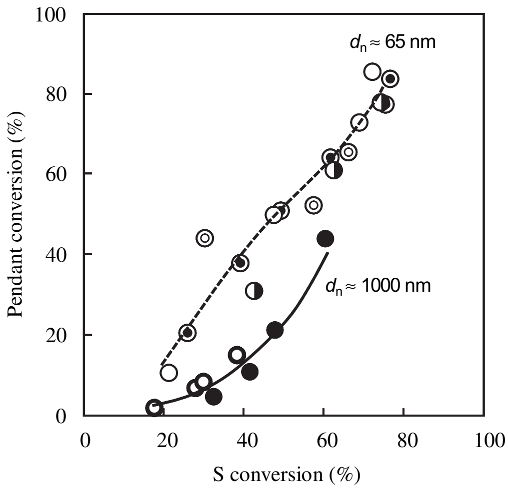

Fig. 4. Pendant conversions for TEMPO-mediated radical copolymerization of S and DVB (1 mol%) in miniemulsion at 125 °C at various PS–TEMPO macroinitiator concentrations as indicated. The legend is the same as in Fig. 1.

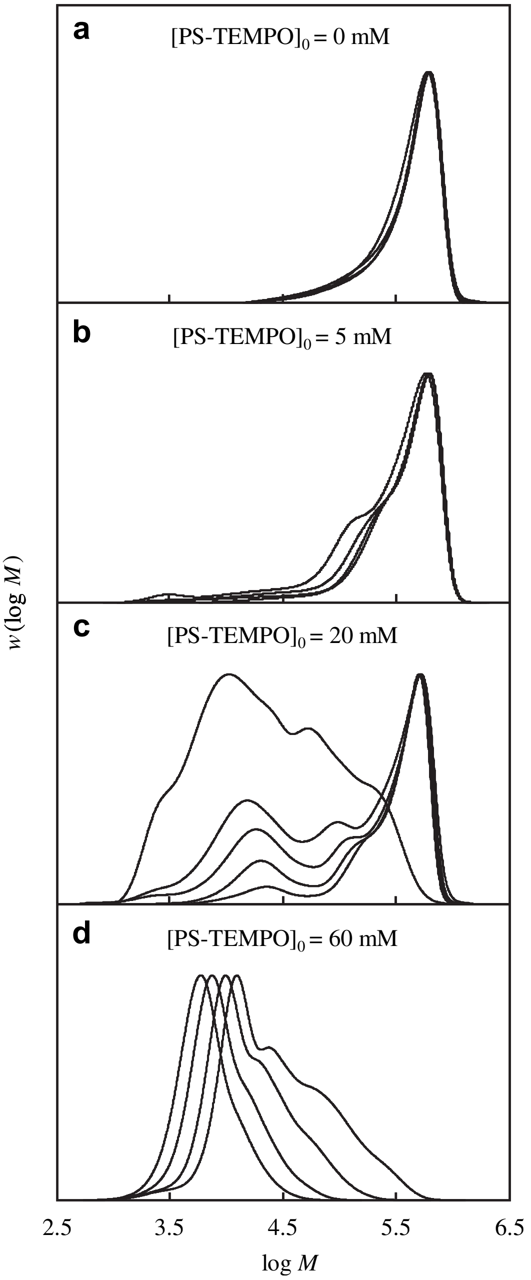

Fig. 5. MWDs normalized to peak height for TEMPO-mediated miniemulsion copolymerization of S and DVB (1 mol%) at 125 °C: (a) [PS–TEMPO]$_0$ = 0 M ($d_n \approx 64$ nm; conv = 24, 46, 74, 86, 95%); (b) [PS–TEMPO]$_0$ = 5 mM ($d_n \approx 65$ nm; conv = 17, 35, 46, 73, 83%); (c) [PS–TEMPO]$_0$ = 20 mM ($d_n \approx 65$ nm; conv = 17, 29, 50, 64, 73%); (d) [PS–TEMPO]$_0$ = 60 mM ($d_n \approx 56$ nm; conv = 28, 42, 46, 56, 63%).

3.4. Molecular weight distributions

Fig. 5 shows the MWDs corresponding to the miniemulsion polymerizations with $d_n \approx 65$ nm in Figs. 1 and 2 (these MWs are linear polystyrene equivalents and are thus underestimated due to branching/crosslinking). It is immediately apparent that there is a very strong dependence of the MWD on [PS–TEMPO]$_0$. In the absence of specific heterogeneous effects on the polymerization, one would expect an increase in [PS–TEMPO]$_0$ to result in lower MW and lower crosslink density due to the reduction in primary chain length. Qualitatively, this is what is observed in Fig. 5.

In the absence of PS–TEMPO (Fig. 5a), one has obviously a conventional non-living radical miniemulsion polymerization initiated by spontaneous radical generation [27]. Interestingly, the MWDs are largely independent of conversion, and in fact very similar to the MWDs obtained with [PS–TEMPO]$_0$ = 5 mM (Fig. 5b). The polymerization with the highest macroinitiator concentration, [PS–TEMPO]$_0$ = 60 mM (Fig. 5d), proceeded with the usual characteristics of a crosslinking CLRP [2,3,41,42], where the MWD reveals a sharp low MW peak corresponding to the primary chains, and a gradually more pronounced high MW shoulder due to crosslinking. The system with [PS–TEMPO]$_0$ = 20 mM exhibits intermediate behavior.

In the polymerization with [PS–TEMPO]$_0$ = 20 mM, the MWD is very broad at 17% S conversion (the MWD at the lowest conversion in Fig. 5c), with MWs spanning from 10^3 to $>10^5$ g mol^{-1}. At 17% S conversion, the primary chain length would be ~7500 g mol^{-1} based on a controlled/living process, and at this point the DVB conversion is ~29% and the pendant conversion ~10% (approximated from Figs. 2 and 4). It follows that each chain of MW ~7,500 g mol^{-1} would possess on the average ~0.12 reacted pendants, which may have reacted intra- or intermolecularly (only intermolecular reaction leads to an increase in MW). In the present system, approximately half of the crosslinks are intermolecular [8], resulting in ~0.06 intermolecular crosslinks per primary chain. With such a low number of reacted pendant unsaturations per chain, the MWD would be narrow, and closely ressemble that of the primary chains. In Fig. 5c at 17% S conversion, it is immediately obvious that this is not the case, but that the system contains a significant amount of crosslinking with the presence of polymer of MW as high as 10^5 g mol^{-1}. Theory dictates that gelation occurs when the number of intermolecular crosslinks per primary chain equals 0.5 [43,44], whereas recent data on crosslinking CLRP suggests 1 crosslink per chain is the requirement [10,45,46].

The main reason that the level of crosslinking is so much higher than predicted based on the polymerization proceeding in a controlled/living fashion is the interface effect on deactivation [22–25]. In the absence of DVB, the present system ($d_n \approx 65$ nm, [PS–TEMPO]$_0$ = 20 mM) proceeds with essentially no livingness, with the MW of the polymer formed remaining close to constant with increasing conversion at $M_n \approx 4.5 \times 10^4$ g mol^{-1} [22]. Following the simple calculations above, it can be estimated that if the primary chain length at 17% conversion is increased from 7,500 to 4.5×10^4 g mol^{-1}, the number of intermolecularly reacted pendant unsaturations per primary chain would increase from 0.06 to approximately 0.36. This value is not high enough to cause gelation (see above), but it is consistent with a high MW with very broad MWD as obtained experimentally (Fig. 5c). It is also likely that enhanced spontaneous radical generation [27] would contribute to the loss of livingness.

As explained in connection with Fig. 1, the magnitude of the interface effect on deactivation and the effect of enhanced spontaneous radical generation both increase with decreasing [PS–TEMPO]$_0$. Both of these effects lead to a reduction in livingness with decreasing [PS–TEMPO]$_0$. In other words, the influence of the interface effect on deactivation as well as enhanced spontaneous radical generation on the crosslinking process would increase with decreasing [PS–TEMPO]$_0$. The value of [PS–TEMPO]$_0$ thus not only influences the crosslinking process via its effect on the primary chain length through $M_{n,th}$ based on an ideal controlled/living process, but also indirectly via the influence of [PS–TEMPO]$_0$ on the extent of the interface effect on the deactivation reaction and enhanced spontaneous radical generation.

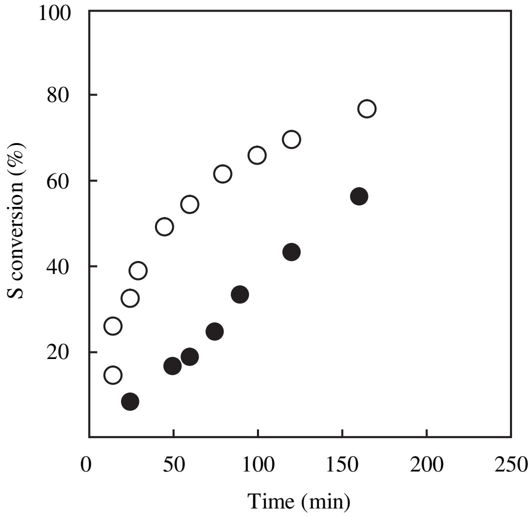

Fig. 6. Conversion-time plots based on S for TEMPO-mediated miniemulsion copolymerization of S and DVB (1 mol%) at 125 °C using [PS–TEMPO]$_0$ = 20 mM without free TEMPO (○; d_n = 65 nm, d_w = 85 nm) and with 5 mol% free TEMPO (rel. to PS–TEMPO) (●; d_n = 66 nm, d_w = 89 nm).

3.5. Addition of free nitroxide

In order to confirm the influence of the interface effect on deactivation and enhanced spontaneous radical generation on the crosslinking process, miniemulsion NMP with [PS–TEMPO]$_0$ = 20 mM was repeated in the presence of 5 mol% free TEMPO relative to PS–TEMPO. It has previously been shown for the corresponding system without DVB that this leads to good control/livingess in cases where poor control/livingness is caused by the interface effect [23], i.e. the effects of the interface on the polymerization via the interface effect on

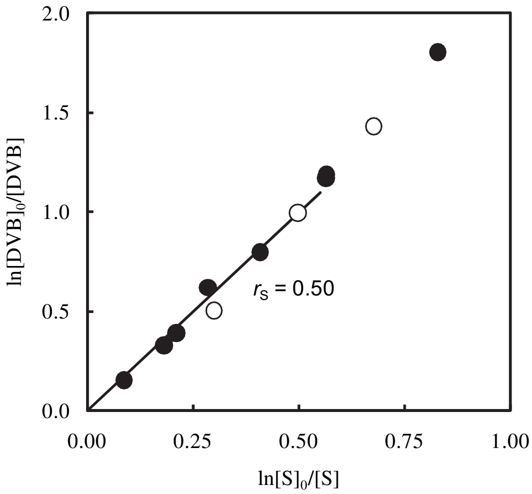

Fig. 7. Relative rates of S and DVB consumption expressed as ln[DVB]$_0$/[DVB] vs. ln[S]$_0$/[S] for TEMPO-mediated copolymerization of S and DVB (1 mol%) at 125 °C in miniemulsion using [PS–TEMPO]$_0$ = 20 mM without free TEMPO (○; d_n = 65 nm) and with 5 mol % free TEMPO (rel. to PS–TEMPO) (●; d_n = 66 nm).

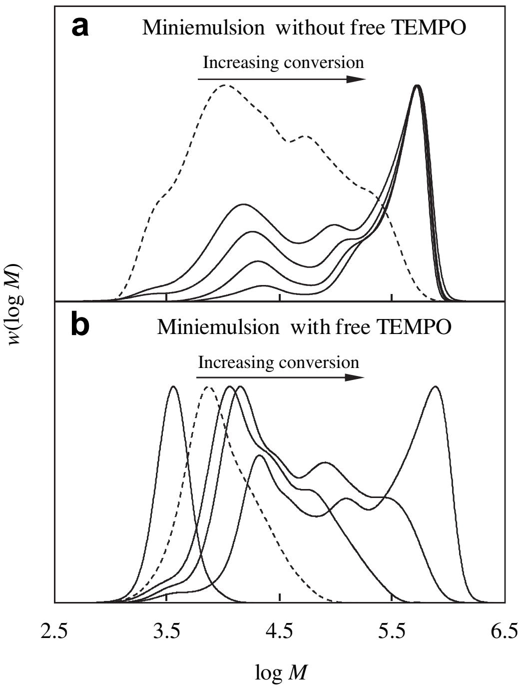

Fig. 8. MWDs (normalized to peak height) at various conversions for TEMPO-mediated miniemulsion copolymerization of S and DVB with $[\text{PS–TEMPO}]_0 = 20$ mM at 125 °C (a) without free TEMPO ($d_n = 65$ nm; conv = 17, 29, 50, 64, 73%) and (b) with 5 mol% free TEMPO (rel. to PS–TEMPO) ($d_n = 66$ nm; conv = 8, 17, 19, 25, 34, 56%). The dotted lines are MWDs at 17% conversion.

deactivation and enhanced spontaneous initiation are significantly reduced/eliminated by addition of free TEMPO. The polymerization proceeded at a markedly lower rate in the presence of free TEMPO as anticipated (Fig. 6).

The rate of DVB consumption relative to S consumption was unaffected by free TEMPO, with $r_S = 0.50$ both with and without free TEMPO (Fig. 7). Fig. 8 shows the MWDs at various conversions with and without free TEMPO. The MWDs at low to intermediate conversion are narrower and of lower average MW with free TEMPO than without. At 17% S conversion, the MWD obtained in the presence of free TEMPO is close to monomodal with only a slight shoulder on the high MW side due to intermolecular reaction of pendant unsaturations, which is in sharp contrast to the very broad and multimodal MWD at the same S conversion in the absence of free TEMPO. The difference between the two MWDs (for any sets of MWDs at same/similar S conversion) originates in the effect of the interface effect on deactivation and enhanced spontaneous radical generation on the polymerization process. If these effects were negligible, one would expect the MWDs with and without free TEMPO to be very similar.

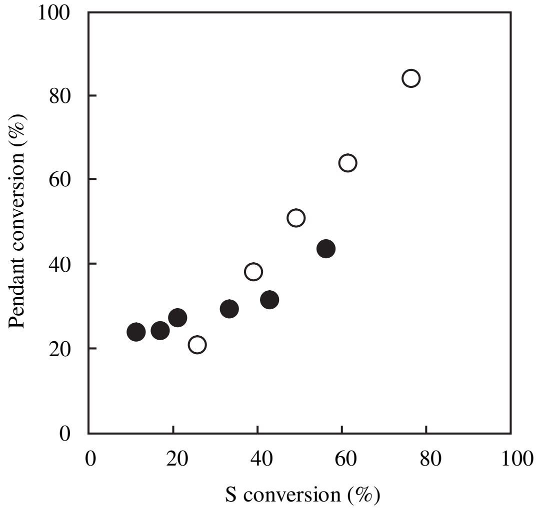

Fig. 9. Pendant conversions vs. S conversion for TEMPO-mediated miniemulsion copolymerization of S and DVB (1 mol%) at 125 °C using $[\text{PS–TEMPO}]_0 = 20$ mM without free TEMPO (○; $d_n = 65$ nm) and with 5 mol % free TEMPO (rel. to PS–TEMPO) (●; $d_n = 66$ nm).

The pendant conversions were similar with and without free TEMPO (Fig. 9), although it appeared that the presence of free TEMPO led to a slight increase in pendant conversion at low S conversion, and a minor decrease in the intermediate S conversion range.

4. Conclusions

Nitroxide-mediated radical copolymerization of styrene (99 mol%)/divinylbenzene (1 mol%) employing the nitroxide 2,2,6,6-tetramethylpiperidinyl-1-oxy (TEMPO) in aqueous miniemulsion using sodium dodecylbenzenesulfonate as surfactant has been investigated at 125 °C. The degree of crosslinking at a given styrene conversion increases with decreasing $[\text{PS–TEMPO}]_0$ significantly more than what would be anticipated based solely on the increase in primary chain length assuming an ideal controlled/living process. By use of polymerizations with added free TEMPO, it is shown that this discrepancy has its origin in the oil–water interface effect on the deactivation reaction between propagating radicals and TEMPO. This interface effect refers to how some fraction of TEMPO is located near/adsorbed at the interface, leading to a reduction in deactivation rate, higher polymerization rate and (partial) loss of control/livingness. The interface effect causes a marked increase in primary chain length, and consequently a concomitant increase in the number of crosslinks per primary chain. Polymerizations in the presence of free TEMPO minimizes the interface effect, and one then obtains molecular weight distributions as expected based on a controlled/living process.

The present results have shown that the oil–water interface can exert significant influence on network formation during crosslinking NMP in aqueous miniemulsion. A thorough understanding of such phenomena is essential for tailored synthesis of nanogels for a variety of applications.

Acknowledgements

This work was supported by a Grants-in-Aid Program Grant (19550125) from the Japan Society for the Promotion of Science (JSPS), a Kobe University Takuetsu-shita Research Project Grant, and a Monbukagakusho (MEXT scholarship) from the Ministry of Education, Science, Sports, and Culture of Japan.

References

[1] Braunecker WA, Matyjaszewski K. Prog Polym Sci 2007;32:93–146.
[2] Zetterlund PB, Kagawa Y, Okubo M. Chem Rev 2008;108:3747–94.
[3] Gao HF, Matyjaszewski K. Prog Polym Sci 2009;34:317–50.
[4] Ide N, Fukuda T. Macromolecules 1997;30:4268–71.
[5] Ide N, Fukuda T. Macromolecules 1999;32:95–9.
[6] Zetterlund PB, MdN Alam, Minami H, Okubo M. Macromol Rapid Commun 2005;26:955–60.
[7] Norisuye T, Morinaga T, Tran-Cong-Miyata Q, Goto A, Fukuda T, Shibayama M. Polymer 2005;46:1982.
[8] MdN Alam, Zetterlund PB, Okubo M. Macromol Chem Phys 2006;207:1732–41.
[9] Tanaka T, Suzuki T, Saka Y, Zetterlund PB, Okubo M. Polymer 2007;48: 3836–43.
[10] Gao H, Min K, Matyjaszewski K. Macromolecules 2007;40:7763–70.
[11] Li WW, Gao HF, Matyjaszewski K. Macromolecules 2009;42:927–32.
[12] Tao L, Liu JQ, Tan BH, Davis TP. Macromolecules 2009;42:4960–2.

[13] Oh JK, Drumright R, Siegwart DJ, Matyjaszewski K. Prog Polym Sci 2008;33:448–77.

[14] Georges MK, Veregin RPN, Kazmaier PM, Hamer GK. Macromolecules 1993;26:2987–8.

[15] Hawker CJ, Bosman AW, Harth E. Chem Rev 2001;101:3661–88.

[16] Charleux B, Nicolas J. Polymer 2007;48:5813–33.

[17] Cunningham MF. Prog Polym Sci 2008;33:365–98.

[18] Zetterlund PB, Okubo M. Macromolecules 2006;39:8959–67.

[19] Zetterlund PB, Okubo M. Macromol Theory Simul 2007;16:221–6.

[20] Maehata H, Buragina C, Cunningham M, Keoshkerian B. Macromolecules 2007;40:7126–31.

[21] Zetterlund PB, Okubo M. Macromol Theory Simul 2009;18:277–86.

[22] Nakamura T, Zetterlund PB, Okubo M. Macromol Rapid Commun 2006;27:2014–8.

[23] Zetterlund PB, Nakamura T, Okubo M. Macromolecules 2007;40:8663–72.

[24] MdN Alam, Zetterlund PB, Okubo M. J Polym Sci Part A Polym Chem 2007;45:4995–5004.

[25] MdN Alam, Zetterlund PB, Okubo M. Polymer 2008;49:3428–35.

[26] Lin M, Hsu JCC, Cunningham MF. J Polym Sci Part A Polym Chem 2006;44:5974–86.

[27] MdN Alam, Zetterlund PB, Okubo M. Polymer 2008;49:883–92.

[28] Zetterlund PB, MdN Alam, Okubo M. Polym J 2008;40:298–9.

[29] Saka Y, Zetterlund PB, Okubo M. Polymer 2007;48:1229–36.

[30] Zetterlund PB, Saka Y, Okubo M. Macromol Chem Phys 2009;210:140–9.

[31] Okubo M, Konishi Y, Minami H. Progr Colloid Polym Sci 2003;124:54–9.

[32] Okubo M, Minami H. Colloid Polym Sci 1997;275:992–7.

[33] Konishi Y, Okubo M, Minami H. Colloid Polym Sci 2003;281:123–9.

[34] Okubo M, Minami H, Yamashita T. Macromol Symp 1996;101:509–16.

[35] Goto A, Fukuda T. Prog Polym Sci 2004;29:329–85.

[36] Greenley RZ. Free radical copolymerization reactivity ratios. In: Brandrup J, Immergut EH, Grulke EA, editors. Polymer handbook. John Wiley & Sons; 1999. p. II/181.

[37] Ryan J, Aldabbagh F, Zetterlund PB, Yamada B. React Funct Polym 2008;68:692–700.

[38] Alam MdN, Zetterlund PB, Okubo M. Polymer 2009;50:1632–6.

[39] Keskinel M, Okay O. Polym Bull 1998;40:491.

[40] Landin DT, Macosko CW. Macromolecules 1988;21:846–51.

[41] Li Y, Armes SP. Macromolecules 2005;38:8155–62.

[42] Wang AR, Zhu S. J Polym Sci Part A Polym Chem 2005;43:5710–4.

[43] Stockmayer WH. J Chem Phys 1944;12:125.

[44] Flory P. Principles of polymer chemistry. Ithaca, New York: Cornell University Press; 1953.

[45] Isaure F, Cormack PAG, Graham S, Sherrington DC, Armes SP, Buetuen V. Chem Commun 2004;1138.

[46] Bannister I, Billingham NC, Armes SP, Rannard SP, Findlay P. Macromolecules 2006;39:7483.